Integrated Mach-Zehnder based spectral amplitude OCDMA on a passive optical network

Integrated Mach–Zehnder-Based Spectral Amplitude OCDMA on a Passive Optical Network

B. Huiszoon, *Student Member, IEEE*, L. M. Augustin, *Student Member, IEEE*, E. A. J. M. Bente, *Member, IEEE*, H. de Waardt, *Member, IEEE*, G. D. Khoe, *Fellow, IEEE*, M. K. Smit, *Fellow, IEEE*, and A. M. J. Koonen, *Fellow, IEEE*

***Abstract*—In this paper, we present our results on Mach–Zehnder-based spectral amplitude encoded optical code-division multiple access (OCDMA) in a passive optical network using a novel parallel spectral encoder/decoder. The modular construction of orthogonal code processors is shown along with operational settings. Simulation results are shown for an eight-user network scenario. The monolithic integration of a parallel encoder in an InP/InGaAsP material system is discussed whereafter static measurement results are given. Finally, several options are discussed to increase network flexibility and optical transparency.**

***Index Terms*—Code division multiaccess, optical components, optical fiber communication, parallel processing, passive circuits.**

I. Introduction

OPTICAL code-division multiple access (OCDMA) has many attractive features such as cost efficiency, asynchronous access, the resilience against eavesdropping and interference, and soft capacity degradation [1]. One of the applications of OCDMA is communication on passive optical networks (PONs). OCDMA has a powerful natural fit on PON because both are based on broadcast-and-select. As such, optimal sharing of optical medium and carrier is obtained. A PON shared-fiber architecture is envisaged to provide optical transparency in the access network layer, or even beyond, until the personal area network (PAN) of a mobile subscriber [2], [3]. Using OCDMA on multiple wavelength channels in a PON allows code (re)usage per wavelength channel. This offers huge bandwidths to a large number of subscribers for reduced infrastructure costs. The integration of optics herein is the key for a further reduction in hardware complexity, and capital and operational expenditures (CAPEX and OPEX). Many flavors exist in OCDMA that can be differentiated by source (coherent or incoherent), coding domain (time, frequency, or time and frequency), implementation (free space, fiber based, or integrated), and polarity (unipolar or polar). In most coherent systems, short pulses are used, which require expensive sources. We consider incoherent spectral amplitude encoded OCDMA (SAE OCDMA) employing a broadband source and polar signaling. Incoherent sources such as LEDs are cost effective and give a good performance in SAE OCDMA, especially when forward error correction (FEC) is applied [4]. Polar signaling has a 3 dB SNR advantage over unipolar signaling [5]. Here, two complementary fringe patterns are used to represent both the user and the data on the network, i.e., they are used as modulation format and as multiple access mechanism. The coding is performed at the bit rate that limits the receiver bandwidth. As a result, additional cost efficiency is obtained with respect to time-domain encoding where high chip rates are used. Using two complementary fringe patterns is denoted as spectral shift keying (SSK). SSK has also been referred to as complementary spectral keying or recently as code-shift keying for a coherent OCDMA system [6]. A polar SAE OCDMA transmitter may use SSK. A polar receiver is constructed by a decoder with balanced detection at its outputs.

An integrated Mach–Zehnder interferometer (MZI) based polar transmitter is considered in this paper. A polar transmitter efficiently uses the properties of the polar receiver [7]. The integration of optical functions enables large-scale mass production and deployment. An integrated polar transmitter is, therefore, more attractive than, for example, a fiber-based unipolar transmitter shown in [8]. A fiber-based solution is bulky, more expensive, and less stable compared to its integrated counterpart. Additionally, we consider monolithic integration in the InP/InGaAsP material system because it allows integration of passive and active components such as a semiconductor optical amplifier (SOA) [9]. To the best of the authors' knowledge, solutions only in silicon have been demonstrated so far [10]–[12]. We have designed a parallel spectral en/decoder (E/D) that uses only a single optical source to simultaneously generate or process a multitude of encoded optical spectra. A significant reduction in cost and hardware complexity is achieved when a single device is used.

In this paper, we discuss in detail the architecture and the performance of integrated MZI-based SAE OCDMA on a PON. We present the design and implementation of the parallel spectral E/D. The SAE OCDMA PON architecture is then simulated including the parallel spectral E/D at the optical line termination (OLT) side. Results are discussed for upstream and downstream traffic in case of eight possible users. Then, a successful integration in InP/InGaAsP is shown, which shows proof of concept. Finally, we discuss node integration, network reconfigurability based on dynamic wavelength assignment, all-optical routing, and colorless optical network units (ONUs), and a code-sense medium access control (MAC) to introduce robust network flexibility and optical transparency.

Manuscript received December 1, 2006; revised July 13, 2007. This work was supported in part by the Netherlands Organisation for Scientific Research (NWO) under the National Research Combination (NRC) Photonics Research grant and in part by the European Commission. This work was performed under the COBRA SWOOSHING project supported by the IST-MUFINS project.

The authors are with COBRA Institute, Technische Universiteit Eindhoven (TU/e), NL-5600MB Eindhoven, The Netherlands (e-mail: b.huiszoon@tue.nl; secretariaat.tte@tue.nl).

Digital Object Identifier 10.1109/JSTQE.2007.904573

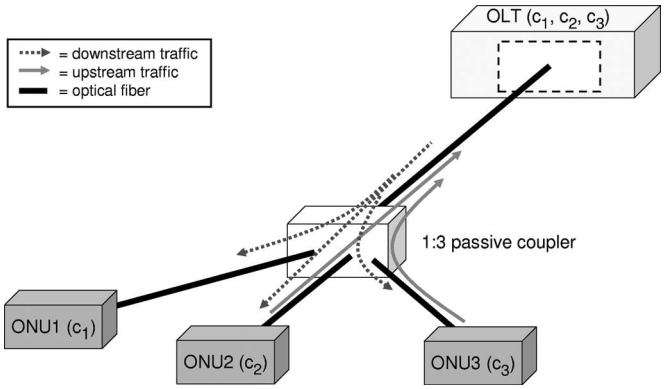

Fig. 1. Basic three-user OCDMA PON scenario.

The paper is organized as follows. First, the envisioned SAE OCDMA PON architecture is briefly introduced in Section II. Then, in Section III, basic building blocks are presented to modularly construct various types of E/Ds of any size. An SAE OCDMA PON eight-user network scenario is simulated in Section IV for the up and downstream case. Section V briefly describes the integration of a one-stage parallel spectral E/D. Finally, a discussion and the conclusions are given in Section VI.

II. Mach-Zehnder-Based SAE OCDMA on PON

The MZI-based solution has a number of properties that are advantageous in SAE OCDMA. The structure can be on the same photonic integrated chip (PIC) together with the source, modulator, filters, and many other functionalities. This results in cost-effective node designs. The MZI as a passive and low-complexity structure also contributes to this. An MZI is reciprocal; thus, a single device or design can be used for encoder and decoder. Here, it is referred to as E/D because it can perform both encoding and decoding operations. The two complementary fringe patterns required in SSK are generated by a single E/D. Finally, large E/Ds generate very complicated fringe patterns that enhance the security of data transmission with spectral amplitude coding.

A Mach–Zehnder-based E/D combination was used in a 100 Mbit/s point-to-point transmission link in [10]. However in a PON, point-to-multipoint transmission is performed. The data streams of multiple ONUs have to be transmitted from and detected at the OLT. This implies that all codes should instantly be available whenever there are data to transmit in order to maintain the asynchronous aspect of using optical codes on PON. Then, according to the state-of-the-art, this requires M banks of encoders and decoders with M sources to basically have M point-to-point transmission links deployed on PON. A significant reduction in hardware complexity is achieved when these M banks of E/Ds are transformed into one single device using one single source. We refer to such a device as a parallel E/D that is introduced in the next section. A three-user OCDMA PON scenario is shown in Fig. 1 in which all three codes have to be available at the OLT. Two different sources and two different SSK transmitters may be used at the ONU side, namely an electrooptic switch in combination with a superluminescent LED (SLED) and a bandpass filter (BPF) or a balanced transmitter

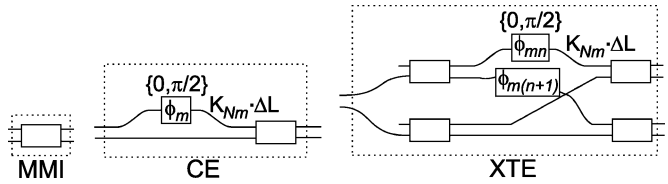

Fig. 2. Three basic building blocks for Mach–Zehnder-based E/Ds.

with SLEDs and BPFs. Either of these combinations ensure the user data are SSK modulated at the outputs of the encoder. The parallel encoder at the OLT side uses an SLED and BPF in combination with electrooptic switches such that each ONU receives its own data. However, a balanced transmitter can be used to broadcast messages or data to all ONUs. The optical codes should be decorrelated not only by optical delay lines but also by polarization. All BPFs have a passband of the size of the free spectral range (FSR) of the E/Ds. The source and BPF should be as flat as possible to have negligible effect on the shape of the optical code. A booster amplifier should not be used because it will affect the optical code by amplified spontaneous emission (ASE) noise. A Mach–Zehnder-based SAE OCDMA PON architecture with these characteristics is discussed in detail in the following sections.

III. Orthogonal Spectral En/Decoders

A basic MZI generates two complementary spectra. A second set can be generated by applying an extra frequency-independent $\pi/2$ phase shift in one of the arms. By doing so, the frequency transfer function is transformed from the cosine to its orthogonal the sine. The orthogonal sets of complementary spectra are denoted as phase codes. The phase codes are binary identified by a 0 when the extra phase shift is absent and by a 1 when the extra phase is present. The resulting binary word is referred to as a phase code identifier (PCI). It is clear that a single MZI can generate only two phase codes. The number of phase codes (or cardinality) of the MZI can be increased by cascading another stage. A parallel spectral E/D (or tree) has been proposed, which is typically placed at the OLT in a PON [13], [14]. Its cost-efficient design uses only a single optical source to simultaneously generate or process a multitude of encoded optical spectra. As such, a significant reduction in cost and hardware complexity is achieved.

Modular construction of E/Ds eases the design; therefore, three building blocks have been defined to construct cascade en tree E/Ds of any size. A 2×2 3-dB multimode interference (MMI) coupler, a 2×2 cascade element (CE), and a 2×4 crossed tree element (XTE) are shown in Fig. 2.

An exact 3 dB coupling ratio is assumed for all couplers. The transmission characteristics of the E/Ds are described according to the propagation matrix [15]. Equation (1) shows the relationship between input $\boldsymbol{E}_{\rm in}$ and output $\boldsymbol{E}_{\rm out}$

$$\boldsymbol{E}_{\rm out} = \boldsymbol{M}\cdot\boldsymbol{E}_{\rm in} \tag{1}$$

with $\boldsymbol{M}$ being the propagation matrix. The power transfer function is then given by

$$\boldsymbol{P}_{\rm out} = |\boldsymbol{M}|^2\cdot\boldsymbol{P}_{\rm in}. \tag{2}$$

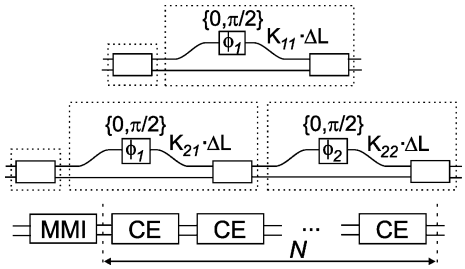

Fig. 3. One-, two-, and N-stage cascade E/Ds.

The propagation matrices $\boldsymbol{M}_{\mathrm{MMI}}$, $\boldsymbol{M}_{\mathrm{CE}}$, and $\boldsymbol{M}_{\mathrm{XTE}}$ of the three building blocks are easily described by [16]

$$\boldsymbol{M}_{\mathrm{MMI}} = \frac{1}{\sqrt{2}} \begin{bmatrix} 1 & j \\ j & 1 \end{bmatrix} \tag{3}$$

$$\boldsymbol{M}_{\mathrm{CE}} = \frac{1}{\sqrt{2}} \begin{bmatrix} h_{\varphi}(\phi_m) & j \\ j h_{\varphi}(\phi_m) & 1 \end{bmatrix} \tag{4}$$

and

$$\boldsymbol{M}_{\mathrm{XTE}} = \frac{1}{2} \begin{bmatrix} j h_{\varphi}(\phi_{mn}) & -1 \\ -h_{\varphi}(\phi_{mn}) & j \\ h_{\varphi}(\phi_{m(n+1)}) & j \\ j h_{\varphi}(\phi_{m(n+1)}) & 1 \end{bmatrix} \tag{5}$$

with $h_{\varphi}(\phi) = e^{-j(\varphi+\phi)}$, $\varphi = 2\pi f n_{\mathrm{eff}} K_{Nm}\, \Delta L/c$, where f is the optical frequency, n_{eff} the effective refractive index of the waveguide, K_{Nm} the multiplication factor at stage m of an N-stage E/D, ΔL the path length difference, c the speed of light, and j the imaginary unit ($j^2 = -1$). The phase shifter ϕ in $h_{\varphi}(\phi)$ represents ϕ_m in case of a CE, and ϕ_{mn} and $\phi_{m(n+1)}$ in case of an XTE with n the odd branch counter ($n = 1, 3, \ldots$). The setting of the phase shifter depends on its position with respect to the PCI. For example, the modular construction of one-, two-, and N-stage cascade E/Ds is shown in Fig. 3. The PCI and the values of K_{Nm} determine the phase code orthogonality for cascade E/Ds. In original work of [10], the cardinality increases by 2^N with N the number of stages, and the path length difference of each stage is the double of the path length difference of the previous stage. A detailed study toward orthogonality in cascade structures has been shown in [17], and has been described in full detail in [18]. The study proved mathematically that the original assumptions do not provide a full set of phase codes. Improved sets of multiplication factors and PCIs have been proposed. Tables I and II show sets for cascade E/Ds up to six stages. Table I shows that the code cardinality increases only for even values of N, except for $N = 1$. If this is applied to tree E/Ds, full binary trees with more than two stages generate redundant phase codes. As a result, a loss in optical power has to be taken into account. A revised method has been proposed to construct trees that generate only orthogonal phase codes [16]. Such trees are constructed by using all three basic building blocks. The XTEs are used until the structure reaches the correct cardinality and the CEs are then used to extend the tree up to the correct length of the PCI. This is of course true only for trees larger than two stages. If the code cardinality C_p is a power of 2, the number of XTE and CE stages of the trees is given by N_{XTE} and N_{CE} according to

$$N_{\mathrm{XTE}} = \log_2(C_{\mathrm{p}}) \tag{6}$$

and

$$N_{\mathrm{CE}} = \begin{cases} 0, & \text{if } N_{\mathrm{XTE}} = 1 \\ N_{\mathrm{XTE}} - 2, & \text{if } N_{\mathrm{XTE}} \neq 1 \end{cases} \tag{7}$$

where $N_{\mathrm{CE}}, N_{\mathrm{XTE}} \in \mathbb{N}$. The total number of stages N equals to $N_{\mathrm{XTE}} + N_{\mathrm{CE}}$. Fig. 4 shows the modular construction of a one-, two-, and N-stage tree to generate C_p phase codes. It has been analyzed that an N-stage tree E/D in Fig. 4 has a direct relationship with an N-stage cascade E/D. As such, both structures generate the same orthogonal phase codes if the settings are applied as listed in Tables I and II. However, each XTE stage gives a 3 dB additional loss and a $\pi/2$ extra phase shift for the upper branch.

TABLE I
PCIs UP TO $N = 6$ [18]

$N=1$	$N=2$	$N=3$	$N=4$	$N=5$	$N=6$
0	**00**	**0x0**	**0000**	**00000**	**000000**
1	**01**	**0x1**	**0001**	**00001**	**000001**
	10	**1x0**	**1000**	**10000**	**000110**
	11	**1x1**	**1001**	**10001**	**000111**
			0110	**00010**	**011000**
			0111	**00011**	**011001**
			1110	**10010**	**011110**
			1111	**10011**	**011111**
					100000
					100001
					100110
					100111
					111000
					111001
					111110
					111111

(*) **The x for $N = 3$ indicates both 0 or 1 may be used**

TABLE II
MULTIPLICATION FACTORS UP TO $N = 6$ [18]

E/D size	$m=1$	$m=2$	$m=3$	$m=4$	$m=5$	$m=6$
$N=1$	**1**	**0**	**0**	**0**	**0**	**0**
$N=2$	**1**	**2**	**0**	**0**	**0**	**0**
$N=3$	**1**	**3**	**5**	**0**	**0**	**0**
$N=4$	**1**	**3**	**7**	**12**	**0**	**0**
$N=5$	**1**	**3**	**7**	**21**	**33**	**0**
$N=6$	**1**	**3**	**7**	**21**	**63**	**96**

IV. SAE OCDMA PON SCENARIOS

We show a PON configuration with the cascade and tree E/Ds at the ONU and OLT side, respectively. The basic network scenario is given in two parts: firstly for upstream and then for

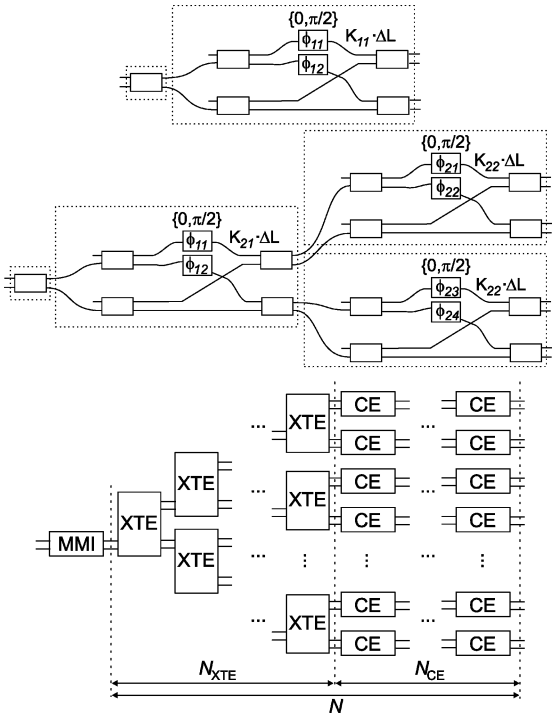

Fig. 4. One-, two-, and N-stage tree E/Ds.

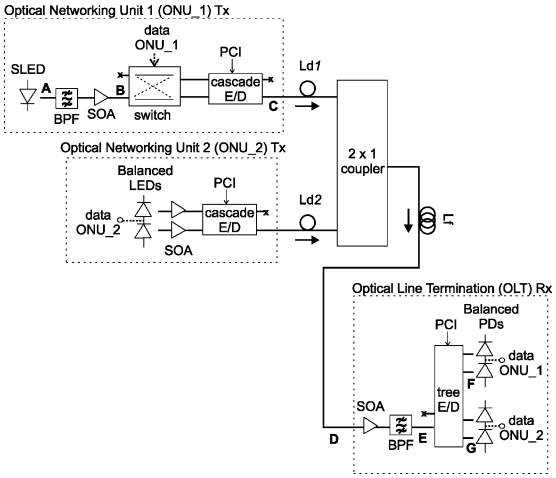

Fig. 5. Upstream SAE OCDMA PON configuration with two users.

downstream communication. The schematics show configurations for only two subscribers. These are easily extended to eight subscribers as used in the simulations.

A. Upstream Mach–Zehnder-Based SAE OCDMA PON

The upstream configuration is shown in Fig. 5 with transmitting ONUs (Tx) and a receiving OLT (Rx). An eight-subscriber scenario is simulated by using the settings of Tables I and II for $N = 4$. An LED is combined with an SOA due to the absence of an SLED module in the simulation software. A fifth-order Bessel BPF with a 3 dB bandwidth of 256 GHz ($\sim$2.1 nm) is used. All SOAs are operated on a bias current of 200 mA. The operating bit rate is 1 Gbit/s. The SSK signals of the ONUs

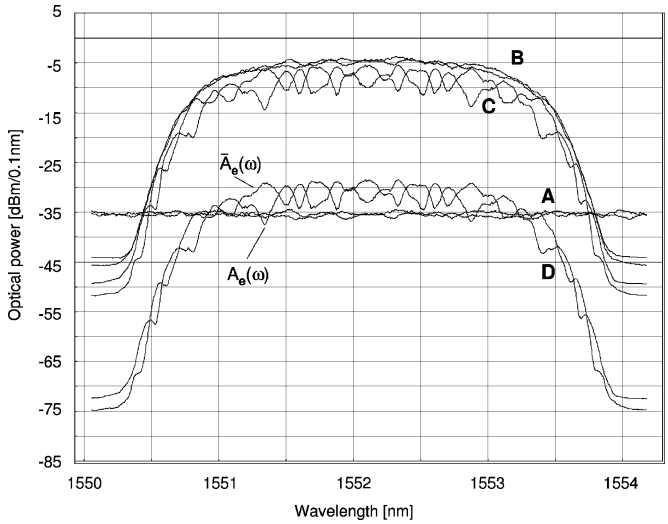

Fig. 6. Optical spectra at various positions in upstream SAE OCDMA PON. (A) SLED. (B) SLED + BPF + AMP. (C) Output cascade. (D) Input tree.

TABLE III
OPTICAL POWER LEVELS FOR UPSTREAM SAE OCDMA PON

	One user [dBm]	Two users [dBm]	Three users [dBm]
A	-18.9		
B	8.7		
C	5.5		
D	-17.5	-14.5	-12.8
E	11.1	12.8	13.6
F	0.3/-2.6	1.5/0.1	2.1/1.3
G	-0.8/-1.0	0.9/0.8	1.7/1.6

(*) **F** properly decodes data stream, **G** is an eavesdropper

are decorrelated by optical delay lines ranging from 2 to 14 ns. To reduce simulation complexity, the optical feeder (L_f) and distribution (L_d) fibers are replaced by attenuators of 10 dB and 4 dB. These values account for connector and transmission losses. At short fiber lengths in the access network, attenuation and dispersion play a minor role. We use a balanced receiver with a trans-impedance amplifier (TIA). After the balanced detection, the electrical signal is filtered by a lowpass filter (LPF) with a cutoff frequency of 938 MHz (gigabit Ethernet filter). A broadband linear gain amplifier then amplifies 15 dB. Finally, a dc level of 150 mV is added to facilitate the visualization of the results. The components of the E/Ds are ideal, i.e., no phase noise or MMI imbalance is taken into account. The influence of phase noise was studied in [18], and was found to have negligible impact on the system if the phase drift is small.

The optical spectra corresponding to Fig. 5 are shown in Fig. 6 for a single transmitting ONU with PCI 0 0 0 0. The figure shows both the fringe pattern $A_e(\omega)$ and its complementary $\bar{A}_e(\omega)$. Average optical power levels at different positions in the setup of Fig. 5 are shown in Table III for three-user cases. The 3 dB loss of the cascade (**B**–**C**) corresponds with the loss at the output of the cascade. Table III shows that the eavesdropper receives equal optical powers that should lead to a zero electrical output. However, the tree output with phase code PCI 0 0 0 0 receives

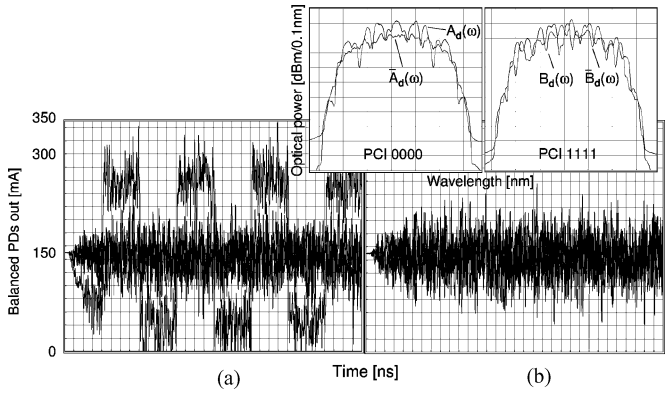

Fig. 7. Electrical output signals at a four-stage tree decoder. (a) ONU 1-4. (b) ONU 5-8 in SAE OCDMA PON. (Inset) Optical output spectra of PCI 0 0 0 0 and PCI 1 1 1 1; upstream scenario.

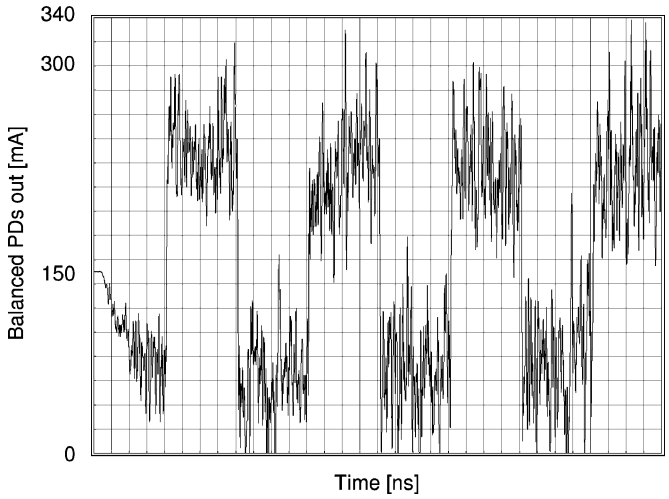

Fig. 8. Decoded bitstream at output PCI 0 0 0 0 of a four-stage tree decoder for two transmitting ONUs with PCI 0 0 0 0 and 0 1 1 0.

high and low optical powers. This leads to a polar electrical output, as shown in Fig. 7(a) and (b) for all eight outputs. The insets show the optical spectrum at outputs PCI 0 0 0 0 (matched) and PCI 1 1 1 1 (nonmatched) if fringe pattern $A_e(\omega)$ in Fig. 6 is received. Table III shows that when multiple users communicate on the network, the performance degrades but the eavesdropper still cannot receive any of the data streams. Unfortunately, a bit error rate measurement could not be realized in the simulation software. The decoded bitstream at the output with PCI 0 0 0 0 in case of an interferer is shown in Fig. 8.

B. Downstream Mach–Zehnder-Based SAE OCDMA PON

The downstream configuration is shown in Fig. 9 with receiving ONUs and a transmitting OLT. Same settings are used for the downstream scenario except the bias currents of the SOAs in Fig. 9. The SOAs at the OLT are operated on a bias current of 250 mA and the SOAs at the ONUs on 150 mA. The higher amplification is required due to the additional loss of 9 dB introduced by the coupling element, which is required at the OLT to multiplex the data streams onto L_f. The optical spectra

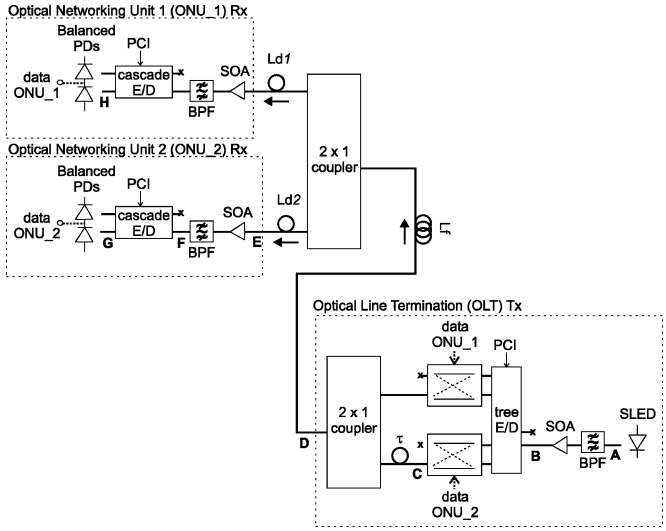

Fig. 9. Downstream SAE OCDMA PON configuration with two users.

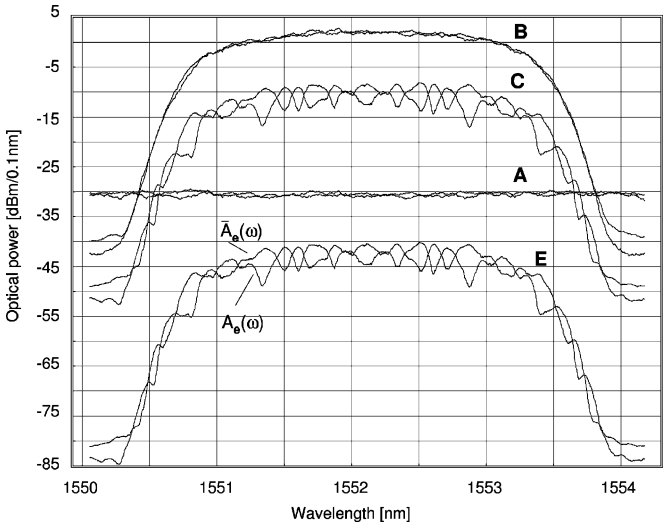

Fig. 10. Optical spectra at various positions in downstream SAE OCDMA PON. (A) SLED. (B) SLED + BPF + AMP. (C) Output tree. (E) Input cascade.

corresponding to Fig. 9 are shown in Fig. 10 for a single data stream from the OLT to the ONUs with PCI 0 0 0 0. Average power levels at different positions in the setup of Fig. 9 are shown in Table IV for three-user cases. The 12 dB loss of the tree encoder (**B–C**) corresponds with the 3×3 dB additional loss of the XTE stages and the 3 dB coupling loss at the output of the tree. The received electrical signals are shown in Fig. 11 for all eight ONUs. The insets show the optical spectrum at outputs PCI 0 0 0 0 (matched) and PCI 1 1 1 1 (nonmatched) if fringe pattern $A_e(\omega)$ in Fig. 10 is received. The decoded bitstream at ONU with PCI 0 0 0 0 in case of an interferer is shown in Fig. 12. Similar results are obtained and compared with those shown in Figs. 7 and 8 even though the received optical power is less.

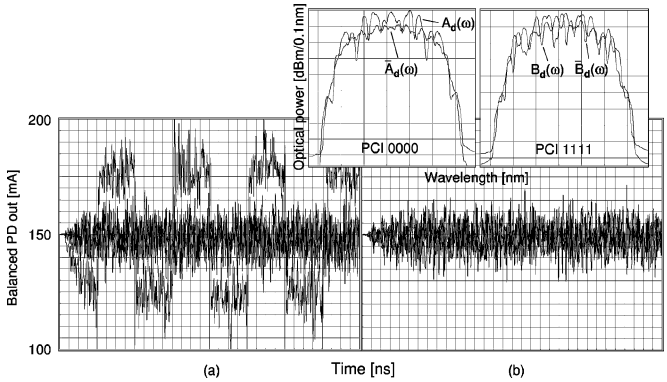

Fig. 11. Electrical output signals at four-stage cascade decoders. (a) ONU 1-4. (b) ONU 5-8 in SAE OCDMA PON. (Insets) Optical output spectra of decoders PCI 0 0 0 0 and PCI 1 1 1 1; downstream scenario.

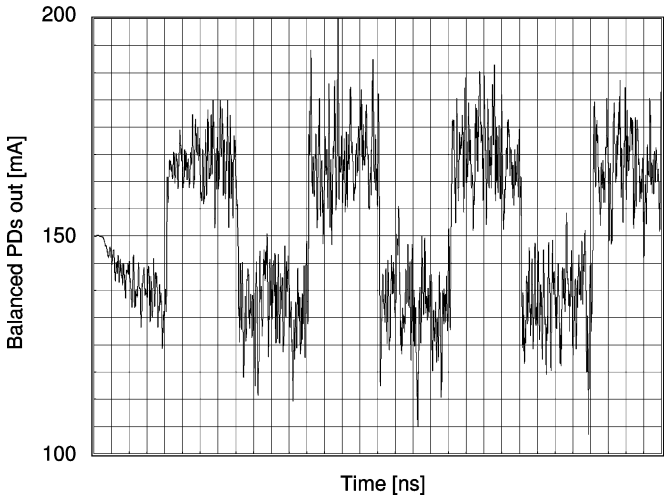

Fig. 12. Decoded bitstream at output PCI 0 0 0 0 of a four-stage cascade decoder for a transmission to ONUs with PCI 0 0 0 0 and 0 1 1 0.

TABLE IV
OPTICAL POWER LEVELS FOR DOWNSTREAM SAE OCDMA PON

	One user [dBm]	Two users [dBm]	Three users [dBm]
A	-14.1		
B	15.1		
C	3.1		
D	-6.0	-2.9	-1.2
E	-29.0	-26.0	-24.2
F	-3.9	-1.1	0.7
G	-5.6/-8.5	-3.3/-4.7	-1.8/-2.8
H	-6.8/-7.0	-3.9/-4.0	-2.2/-2.3

(*) **G** properly decodes data stream, **H** is an eavesdropper

C. Discussion

Figs. 7, 8, 11, and 12 show an unstable behavior with large signal fluctuations during a bit period. This effect is less strong in the time traces shown in Fig. 13 of the similar but continuous wave (unmodulated) back-to-back setup used in [16] to study code orthogonality. However, in the setups shown in Figs. 5 and 9, four ASE sources are cascaded until detection. It is well understood that the incoherent summation of signal powers in the same wavelengths will give rise to excessive fluctuations in the detected power due to the wave nature of light that undergoes constructive and destructive interference [19]. This noise source is referred to as speckle noise and is still present even in the absence of interfering users. The operational settings of the ASE sources could be optimized to suppress the noise, for example, by operating the SOAs under high bias currents in the gain-saturation regime [20]. Choosing a larger optical bandwidth than the simulated 256 GHz will also smoothen out the effects of the speckle noise in the band. In any case, [10] has experimentally shown good performance at 100 Mb/s by using larger, seven-stage cascades with an FSR of 640 GHz ($\sim$5 nm). A large FSR could not be modeled due to computing limitations. Next to optimizing the optical setup, a limiting electrical amplifier with thresholding would also significantly improve the quality of the detected signal.

Hence, the results of the simulations show a limited performance to at most three simultaneous users on the PON, but we observe room for great improvement in the optical and electrical signal-to-noise ratio.

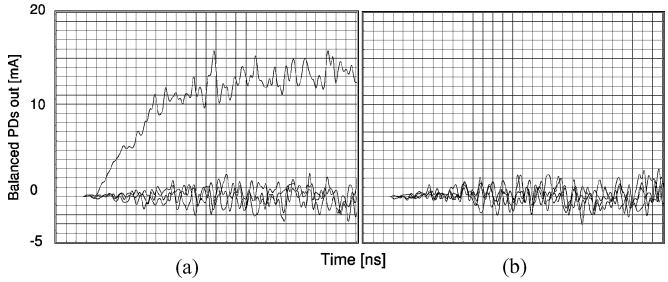

Fig. 13. Continuous wave back-to-back time traces of eight-user case. (a) ONU 1-4. (b) ONU 5-8.

TABLE V
LAYER STACK FOR INTEGRATION OF TREE WITH AN SSC

Material	Thickness [nm]
p^+ InGaAs	100
p^+ InP	1200
i InP	300
Q(1.25)	500
n^- InP	4000
n^+ InP	substrate

V. INTEGRATED ONE-STAGE PARALLEL ENCODER

A one-stage tree is integrated in the InP/InGaAsP material system, which offers the possibility to monolithically integrate the device with active and passive components. The device is fabricated on a layer structure, as shown in Table V.

This stack contains of a waveguide layer of 500-nm-thick undoped InGaAsP with a band gap of 1.25 μm. The top cladding consists of a 300 nm not intentionally doped (n.i.d.) InP and a 1200 nm p^+-doped InP layer. The top contact is a p-InGaAs layer. Below these layers, a 4-μm-thick lowly n-doped InP layer is present, used as a secondary waveguide layer.

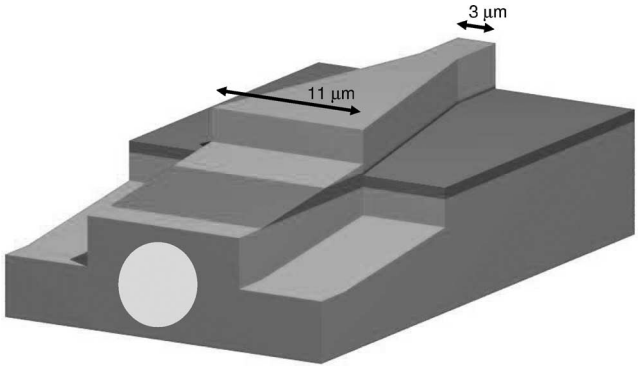

Fig. 14. Schematic of the implemented SSC with an illustrative spot.

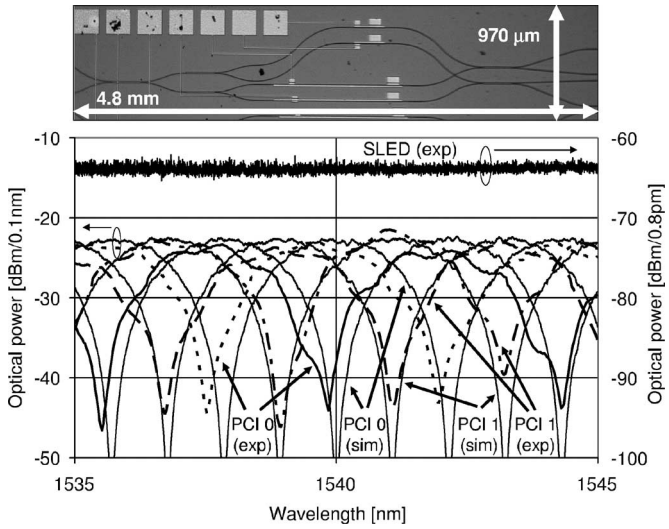

Fig. 15. Microscopic photo of integrated one-stage tree (up) with corresponding fringe patterns (simulation and measurement).

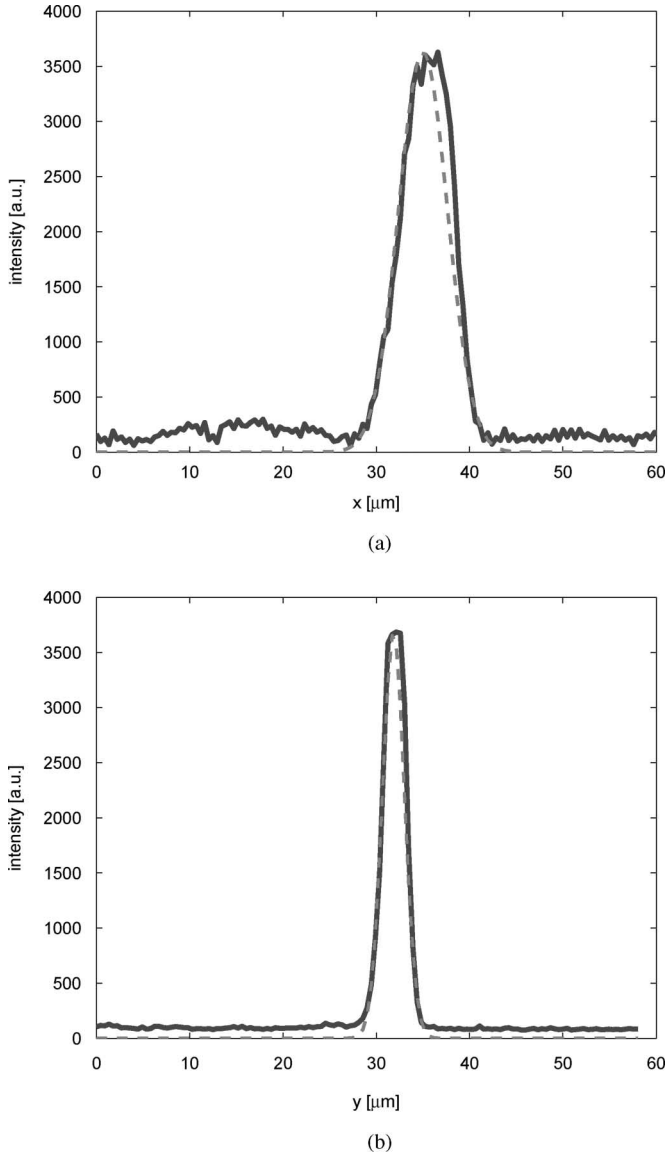

Fig. 16. CCD traces and Gaussian approximate (dashed line) of the SSC output field.

The passive waveguides, the MMI couplers and the electrooptical phase shifters are ridge structures, shallowly etched, 100 nm into the $Q(1.25)$ layer. A spot size converter (SSC) as shown in Fig. 14 is made by tapering the waveguides both laterally and vertically down to the secondary waveguide layer [21], [22]. In this layer, an 11-μm-wide fiber-matched waveguide (FMW) is etched to efficiently couple to a standard single-mode fiber. The phase codes of the integrated tree are measured and show well resemblance with simulated behavior [14]. The integrated chip, and the simulated and measured fringe patterns (FSR $=\sim$5 nm) are shown in Fig. 15. The measured insertion loss is around 10 dB. This accounts for less than 2 dB propagation losses (2.5 dB/cm), 1.5 dB MMI losses, 2×3 dB splitting losses at the XTE and output, and a 1.5 dB SSC loss. The XTE itself has about 5 dB insertion losses. The propagation losses increase with K_{Nm} at higher stages. The tree is TE polarization dependent due to the strong polarization dependency of the Pockels effect in the electrooptic phase shifters.

The SSC performance is further analyzed by using a charge-coupled device (CCD) camera to view the output field. This is plotted in Fig. 16. From these traces, the mode field diameter (MFD) is calculated, which is 10.5 μm in the lateral and 4.7 μm in the vertical direction. From these results, an overlap loss with a single-mode fiber of approximately 1.5 dB is expected. The coupling tolerance to an SMF as a function of the offset is investigated. This results in an alignment tolerance of $\pm$1.5 μm for 1 dB excess loss, as can be seen in Fig. 17. The low overlap and excess loss show a good performance of the designed SSC that enables the chip to be packaged at low fiber-to-fiber insertion losses.

VI. Discussion and Conclusion

The upstream and downstream scenarios in Section IV are easily transformed into a larger bidirectional network scenario because of a large number of shared components. The reciprocal behavior of the E/Ds can be used to integrate the functionalities of the transmitter and receiver at the ONUs. This is simply

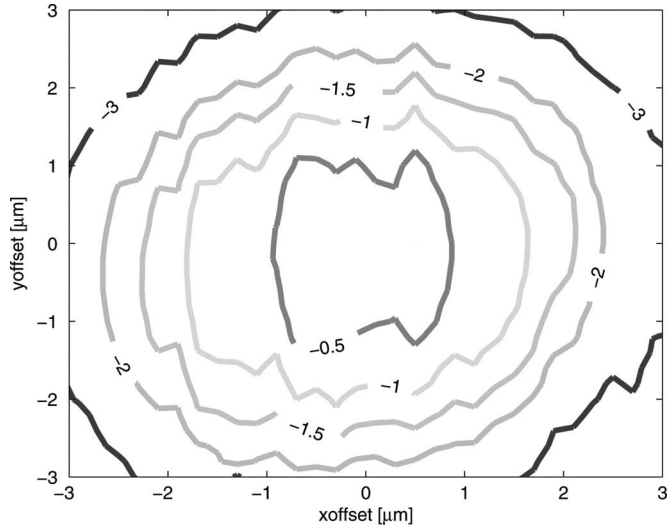

Fig. 17. Coupling tolerance (in decibels) of the SSC to an SMF.

done by adding a coupler stage at the inputs of the cascade E/D to connect the balanced PDs. A separate receiving circuit is required at the OLT in order to maintain truly asynchronous communication on the network. Therefore, a circulator should be used to separate the upstream and downstream channels. The bidirectional node design is fully integrateable in InP/InGaAsP PICs. This is an important advantage of the Mach–Zehnder-based SAE OCDMA solution.

The periodicity of the Mach–Zehnder-based E/Ds can be exploited on the way to wavelength agnostic ONUs. If the BPFs are made tunable, the ONUs can then be placed in any distribution of wavelength channels in the network. Remote wavelength channel delivery from the OLT can be considered to have a colorless ONU. A dynamic wavelength division multiplexing (WDM) scheme can also be applied to allocate capacity. The OLT is not limited to just a single PON, but it may have multiple PONs connected. An increase of optical network transparency is achieved by considering all-optical routing in the subdomain of the OLT. If each PON operates on its own (dynamically) assigned wavelength, all-optical wavelength routing (WR) maximizes the throughput in the CO's subnet of PONs. We aim at no wavelength conversion at the CO to increase the end-to-end optical transparency that also simplifies the network scenario. The SSK signal is transmitted on the wavelength of the destination PON (λ_{out}) by using the optical orthogonal code of the addressee. If the code labeled wavelength channel is routed correctly, the broadcast-and-select properties of PON and OCDMA ensure that the addressee receives its data. A reconfigurable optical add-drop multiplexer (OADM) based on microring resonators has flexible WR functionality [23].

It is clear that a collision may occur at an aggregation point when multiple ONUs simultaneously transmit data to a similar destination. Data not intended for nodes outside the "home" PON are sent on the assigned wavelength (λ_{home}) with the ONU's own optical orthogonal code. Collisions may also occur if direct or peer-to-peer communication is enabled between two ONUs in the same PON. Therefore, a MAC is required to avoid such collision. Code sensing has been analyzed for IP routing in a fiber-Bragg grating (FBG) based SAE OCDMA star network [24]. The transparent deployment of packet-based (Ethernet) services in a Mach–Zehnder-based SAE OCDMA PON system has been proposed in [25]. It is suggested to perform code sensing directly at the transmitter in the optical physical layer (PHY). The Mach–Zehnder-based E/Ds are reciprocal; thus, the existing setup is easily enhanced with a code-sense functionality by adding only few components rather than by adding a separate circuit. The passive node in the PON has to be extended such that power is reflected to "all but own fiber." This implies that a transmitting node cannot sense its own traffic. If another ONU transmits data on the same wavelength channel with the same phase code, a mere peak in the autocorrelation is enough to detect a collision at the transmitter.

We believe that spectral amplitude encoded OCDMA with MZI-based E/D structures is an attractive cost-efficient technique on a PON. We presented a parallel spectral E/D to further reduce network complexity. We have discussed the monolithic integration of node designs in the InP/InGaAsP material system. Simulation results are shown for upstream and downstream eight-user PON scenario. Multiple options have been discussed to increase the flexibility and optical transparency of the architecture.

ACKNOWLEDGMENT

The authors would like to acknowledge the Centre for Integrated Photonics (CIP), Ipswich, U.K., for supplying the wafer for the experiment. They would also like to acknowledge many colleagues for helpful discussions and assistance.

REFERENCES

[1] A. Stok and E. H. Sargent, "The role of optical CDMA in access networks," *IEEE Commun. Mag.*, vol. 40, no. 9, pp. 83–87, Sep. 2002.

[2] A. M. J. Koonen, "Fiber to the home/fiber to the premises: What, where, and when?," *Proc. IEEE*, vol. 94, no. 5, pp. 911–934, May 2006.

[3] B. Huiszoon, E. R. Fledderus, G. D. Khoe, H. de Waardt, and A. M. J. Koonen, "Cost-effective fiber-to-the-PAN architecture based on PON and spectral encoded all-optical CDMA," in *Proc. IET ICAT 2006*, Cambridge, U.K., Jun., pp. 61–64.

[4] S. Ayotte and L. A. Rusch, "A comparison of optical sources for spectral amplitude coding OCDMA," presented at the LEOS Annu. Meeting 2006, Montreal, QC, Canada, Paper ThW5.

[5] L. W. Couch, *Digital and Analog Communication Systems*, 5th ed. Englewood Cliffs, NJ: Prentice-Hall, 1997.

[6] X. Wang, N. Wada, G. Manzacca, G. Cincotti, T. Miyazaki, and K. Kitayama, "Demonstration of 8×10.7 asynchronous code-shift-keying OCDMA with multi-port en/decoder for multi-dimensional optical code processing," presented at the ECOC 2006, Cannes, France, Paper Th3.6.5.

[7] M. Kavehrad and D. Zaccarin, "Optical code-division-multiplexed systems based on spectral encoding of noncoherent sources," *J. Lightw. Technol.*, vol. 13, no. 3, pp. 534–545, Mar. 1995.

[8] J. Penon, S. Ayotte, L. A. Rusch, and S. LaRochelle, "Incoherent SAC OCDMA system at 7×622 Mbps," presented at the CLEO 2006, Long Beach, CA, Paper CWH5.

[9] J. Binsma, R. Broeke, and J. den Besten, "InP-based photonic integration technology," presented at the Tech. Dig. Integr. Photon. Res. (IPR 2004), San Francisco, CA, Jun. 30–Jul. 2, Paper IFB1 (invited).

[10] C. F. Lam, R. Vrijen, D. T. K. Tong, M. C. Wu, and E. Yablonovitch, "Experimental demonstration of spectrally encoded optical CDMA systems using Mach Zehnder encoder chains," presented at the CLEO 1998, San Francisco, CA, May, Paper CThU4.

[11] C. H. Lee, S. Zhong, X. Lin, J. F. Young, and Y. J. Chen, "Planar lightwave circuit design for programmable complementary spectral keying encoder and decoder," *Electron. Lett.*, vol. 35, no. 21, pp. 1813–1815, Oct. 1999.
[12] T. W. Mossberg, D. Iazikov, and C. Greiner, "Planar-waveguide integrated spectral comparator," *J. Opt. Soc. Amer.*, vol. 21, no. 6, pp. 1088–1092, Jun. 2004.
[13] Eindhoven Univ. Technol., Netherlands Patent Application 1031833, May 2006.
[14] B. Huiszoon, L. M. Augustin, R. Hanfoug, L. Bakker, M. J. H. Sander-Jochem, E. R. Fledderus, G. D. Khoe, J. J. G. M. van der Tol, H. de Waardt, M. K. Smit, and A. M. J. Koonen, "Integrated parallel spectral OCDMA en/decoder," *IEEE Photon. Technol. Lett.*, vol. 19, no. 7, pp. 528–530, Apr. 2007.
[15] B. H. Verbeek, C. N. Henry, N. A. Olsson, and K. J. Orlowsky, "Integrated four-channel Mach–Zehnder multi/demultiplexer fabricated with phosphorous doped SiO_2 waveguides on Si," *J. Lightw. Technol.*, vol. 6, no. 6, pp. 1011–1015, Jun. 1988.
[16] B. Huiszoon, L. Bakker, H. de Waardt, G. D. Khoe, E. R. Fledderus, and A. M. J. Koonen, "Orthogonal en/decoders for truly asynchronous spectral amplitude encoded OCDMA," presented at the ICC 2007, Glasgow, U.K., Jun., Session ONS1, Paper 3.
[17] I. Radovanovic, L. Bakker, and W. van Etten, "Improvement in design of Mach–Zehnder en/decoder for implementing new orthogonal codes in OCDMA systems," in *Proc. IEEE CVT Benelux Conf. 2001*, pp. 234–236.
[18] I. Radovanovic, "Optical local area networks: New solutions for fiber-to-the-desk applications," Ph.D. dissertation, Twente Univ., Enschede, The Netherlands, Dec. 2003.
[19] C. F. Lam, "Multi-wavelength optical code-division-multiple-access" Ph.D. dissertation, Univ. Calif., Los Angeles, 1999.
[20] M. Zhao, G. Morthier, and R. Baets, "Aanalysis and optimization of intensity noise reduction in spectrum-sliced WDM systems using a saturated semiconductor optical amplifier," *IEEE Photon. Technol. Lett.*, vol. 14, no. 3, pp. 390–392, Mar. 2002.
[21] F. Soares, F. Karouta, B. Smalbrugge, S. Oei, R. Baets, and M. Smit, "InP-based photonic integrated circuit with WDM switched optical delay lines for true-time-delay beamstearing of a 40 GHz phased-array antenna," in *Proc. 12th Eur. Conf. Int. Opt. (ECIO 2005)*, pp. 129–132.
[22] F. M. Soares, F. Karouta, E. J. Geluk, J. H. C. van Zantvoort, and M. K. Smit, "A compact and fast photonic true-time-delay beamformer with integrated spot-size converters," presented at the IPRA 2006, Uncassville, CT, Paper IMF5.
[23] E. J. Klein, D. H. Geuzebroek, H. Kelderman, G. Sengo, N. Baker, and A. Driessen, "Reconfigurable optical add-drop multiplexer using microring resonators," *IEEE Photon. Technol. Lett.*, vol. 17, no. 11, pp. 2358–2360, Nov. 2005.
[24] Z. Wei and H. Ghafouri-Shiraz, "IP routing by an optical spectral-amplitude-coding CDMA network," *Inst. Electr. Eng. Proc. Commun.*, vol. 149, no. 5, pp. 265–269, Oct. 2002.
[25] B. Huiszoon, H. de Waardt, G. D. Khoe, and A. M. J. Koonen, "On the upgrade of an optical code division PON with a code-sense Ethernet MAC protocol," presented at the OFC 2007, Anaheim, CA, Mar., Paper OWC7.

B. Huiszoon (S'02) was born in Vlissingen, The Netherlands, in 1978. He received the M.Sc. degree in electrical engineering from the Technische Universiteit Eindhoven (TU/e), Eindhoven, The Netherlands, in 2003, where he is currently working toward the Ph.D. degree.

His current research interests include the field of broadband optical access networks, optical code division multiple access, and broadband service delivery. He is currently a Reviewer for the *IET Electronics Letters* and *Optics and Laser Technology*.

Mr. Huiszoon was a member of the first board of the IEEE Lasers and Electro-Optics Society (LEOS) Benelux Student Chapter from November 2004 to May 2007. He is a Reviewer for the IEEE PHOTONICS LETTERS. He received the First Prize for the Best Thesis of 2003 at TU/e in April 2004 (1e Mignot Afstudeerprijs 2004). He is a member of the IEEE LEOS and Communications Society.

L. M. Augustin (S'00) was born in Maastricht, The Netherlands, in 1978. He received the M.Sc. degree in electrical engineering in 2002 from the Technische Universiteit Eindhoven, Eindhoven, The Netherlands, where he is currently working toward the Ph.D. degree in the Opto-Electronic Devices Group, COBRA Research Institute He is currently involved in research on the integration of polarization components with active and passive structures on InP-based material.

E. A. J. M. Bente (M'01) received the M.Sc. degree in physics and the Ph.D. degree in atomic laser spectroscopy from Vrije Universiteit, Amsterdam, The Netherlands, in 1983 and 1989, respectively.

From 1988 to 1994, he was with Urenco Nederland B.V., where he led a research group on laser isotope separation. From 1994 to 1996, he was a Researcher at Vrije Universiteit, where he was engaged in solid-state coherent light sources and isotope separation of stable isotopes. He has also been a Research Team Leader with the Institute of Photonics, University of Strathclyde, Glasgow, U.K., where he was involved in high-power diode-pumped solid-state lasers, passive mode locking, and femtosecond laser machining. Since 2001, he has been an Assistant Professor at the COBRA Research Institute, Technische Universiteit Eindhoven, Eindhoven, The Netherlands, where he is engaged in integrated semiconductor laser systems.

Dr. Bente is a member of the Institute of Physics and the Optical Society of America.

H. de Waardt (M'05–A'06) was born in Voorburg, The Netherlands, in December 1953. He received the M.Sc.E.E. and Ph.D. degrees in electrical engineering from Delft University of Technology, Delft, The Netherlands, in 1980 and 1995, respectively.

In 1981, he joined the Physics Department, PTT Research, Leidschendam, The Netherlands, where he worked on performance issues of optoelectronic devices. In 1989, he joined the Transmission Department, where he was involved in wavelength division multiplexing (WDM) high-bit-rate optical transmission. In 1995, he joined the Technische Universiteit Eindhoven (TU/e), Eindhoven, The Netherlands, as an Associate Professor, where he worked on high-capacity trunk transmission. He coordinated the participation of TU/e in ACTS Upgrade, ACTS BLISS, ACTS APEX, and IST FASHION. He is currently a Project Leader of the National Research Initiative Freeband Broadband Photonics (2004–2008). He is the coauthor of more than 100 conference and journal papers. His current research interests include high-capacity optical transmission and networking, integrated optics, and semiconductor optical amplifiers.

Dr. de Waardt is a member of the IEEE Lasers and Electro-Optics Society.

G. D. Khoe (S'71–M'71–SM'85–F'91) received the Elektrotechnisch Ingenieur degree (*cum laude*) in electrical engineering from the Technische Universiteit Eindhoven, Eindhoven, The Netherlands, in 1971.

He has been engaged in research at the Dutch Foundation for Fundamental Research on Matter (FOM) Laboratory on Plasma Physics, Rijnhuizen. In 1973, he joined the Philips Research Laboratories, where he was involved in the area of optical fiber communication systems. In 1983, he was appointed as part time Professor at the Technische Universiteit Eindhoven, where he became a full Professor in 1994, and is currently

the Chairman of the Department of Telecommunication Technology and Electromagnetics (TTE). Most of his work has been devoted to single-mode fiber systems and components. His current research interests include ultrafast all-optical signal processing, high-capacity transport systems, and systems in the environment of the users. He has more than 40 U.S. patents and has authored and coauthored more than 150 papers, invited papers, and chapters in books. He is one of the founders of the Dutch COBRA University Research Institute. In 2001, he brought four European groups together to start a new international alliance called the European Institute on Telecommunication Technologies (eiTT).

Mr. Khoe has been a member and chairman of technical committees, management committees, and advisory committees of several conferences. He has also been an associate editor, a member of the advisory board, or a reviewer of various journals. In Europe, he is either a participant, an evaluator, an auditor, a program committee member, or a member of the steering committee of the research programs of the European Community and of Dutch National Research Programs. He is one of the three recipients of the prestigious Top Research Institute Photonics Grant that is awarded to COBRA in 1998 by the Netherlands Ministry of Education, Culture and Science. He has served the IEEE Lasers and Electro-Optics (LEOS) organization as European Representative in the BoG, the Vice President (VP) for Finance and Administration, the VP Membership, a Board of Governors (BoG) Elected Member, the President, and a member of the Executive Committee of the IEEE Benelux Section. He was the founder of the LEOS Benelux Chapter. He has been a Fellow of the Optical Society of America (OSA) since 2006 and has received the Micro-Optics/Graded-Index (MOC/GRIN) award in 1997.

M. K. Smit (A'93–M'00–SM'01–F'02) received the M.Sc. and Ph.D. degrees in electrical engineering from Delft University of Technology, Delft, The Netherlands, in 1974 and 1991, respectively.

In 1974, he worked on radar and radar remote sensing, and in 1976, he joined Delft University of Technology, where he became the Leader of the Photonic Integrated Circuits Group in 1994 and a Professor in 1998. In 2002, he joined the Photonic Integrated Circuits Group, Technische Universiteit Eindhoven, Eindhoven, The Netherlands, where he is currently the Leader of the Opto-Electronic Devices Group, COBRA Research Institute. He is the inventor of the arrayed waveguide grating.

Dr. Smit received a Lasers and Electro-Optics Society (LEOS) Technical Award in 1997. Also, in 1997, he was one of the recipients of a research grant to establish the National Research Center on Photonics. He became a Fellow of the IEEE Lasers and Electro-Optics Society in 2002 for contributions in the field of optoelectronic integration.

A. M. J. Koonen (M'00–SM'01–F'07) was born in Oss, The Netherlands, in 1954. He received the M.Sc. degree (*cum laude*) in electrical engineering from the Technische Universiteit Eindhoven, Eindhoven, The Netherlands, in 1979.

In 1979, he joined Philips' Telecommunicatie Industrie, part of which has become Lucent Technologies Network Systems, The Netherlands, since 1984. He worked on high-speed transmission systems and optical fiber systems for hybrid access networks. From 1987 to 2000, he was a Technical Manager in the Forward Looking Work Department, Bell Laboratories, Lucent Technologies Network Systems. From 1991 to September 2000, he was a part-time Professor at the University of Twente, Enschede, The Netherlands, where he was the Chair in Photonic Networks. In September 2000, he joined the Technische Universiteit Eindhoven as a part-time Professor and has been a full-time Professor since January 2001, and is currently the Chair in the Broadband Communication Networks, Telecommunication Technology and Electromagnetics Group, Department of Electrical Engineering.

Prof. Koonen was appointed as Bell Laboratories Fellow in 1999.